Available online at www.sciencedirect.com

SciVerse ScienceDirect

Ceramics International 38 (2012) 1427–1434

CERAMICS INTERNATIONAL

www.elsevier.com/locate/ceramint

Electrostatic charge dependence on surface hydroxylation for different Al_2O_3 powders

Israel Lorite [a,*], M.S. Martín-González [b], J.J. Romero [a], M.A. García [a], Jose. L.G. Fierro [c], Jose. F. Fernández [a]

[a] *Instituto de Cerámica y Vidrio, CSIC, 28049 Madrid, Spain*
[b] *Instituto de Microelectrónica de Madrid, CSIC 28760 Tres Cantos, Madrid, Spain*
[c] *Instituto de Catálisis y Petroleoquímica, CSIC 28049 Madrid, Spain*

Received 6 May 2011; received in revised form 5 September 2011; accepted 8 September 2011
Available online 22 September 2011

Abstract

The effect of surface chemistry on the electrostatic charge in α-Al_2O_3 powders was studied. Net charge and tribo-charge of dry powders were measured by the Faraday double cup procedure. High electrostatic charge values were observed in powders with high surface hydroxylation by IR spectroscopy. The nature of hydroxyl groups at the surface determines the polarity of the electrostatic charge. Mixture of particles having intrinsic electrostatic positive and negative charges follows the lever rule. Dry mixtures of differently charged particles favour the dispersion of smaller particles on the surface of the largest ones. An effective random dispersion was achieved by a low-energy process that allowed preserving the morphology of the supporting and supported particles.

Keywords: Absorption; Infrared; XPS; Double Faraday cup

1. Introduction

Nowadays, the trend to reduce particle size into the nanometre range makes the surface properties of the powders very relevant. In the case of nanopowders, electrostatic forces present a predominant role instead the gravitational one. Static electricity is one of the oldest known physical phenomena and it has been studied for centuries and is nowadays a matter of interest for the scientific community. Electrostatic charging occurs when two materials with neutrally charged surfaces come into contact (<4 Å) and then separate [1]. The materials, due to the contact with different surfaces can acquire so-called tribocharge which has been shown by experimental [2] and theoretical [3] works to present a dependence on the particles size. Tribocharging is a common process during powder handling. In powder handling industries, the existence of non-neutral charged powder and tribocharged powder cause electrostatic discharges and ignition hazards. Thus, an accurate measurement of the charge is needed to avoid the hazards. Static charge can be the origin of adhesion (the joining of surfaces of different composition) and cohesion (adherence of surfaces of identical composition) between small particles. It was proved by computer simulation how static charge may improve the particle deposition on different surfaces [4]. The electrostatic charging of powders [5] produces inadequate flowability that impedes adequate powder mixing. On the contrary, surface charge would help dry coating processes which have potential applications in the particle surface modification for cosmetic, food, painting or ceramics industries [6,7].

To understand the effects of electrostatic charging of fine powder, one of the initial problems to be solved is how to measure the electrostatic charge of such powders. One of the simplest and most effective procedures proposed to evaluate the electrostatic charge is the double Faraday cup [8]. Although the Faraday cup does not distinguish the bipolarity of fine particles, it has been reported a device based on Faraday cup to measure it.

A relationship between particle surface and electrostatic charge is not established yet even though this fact is discussed in electrostatic textbooks [9]. Thus, a correct evaluation of

* Corresponding author.
E-mail address: ilorite@icv.csic.es (I. Lorite).

0272-8842/$36.00
doi:10.1016/j.ceramint.2011.09.024

electrostatic charge would also require a complete characterization of the powder under study and its surface chemical characteristics. By both numerous properties and natural abundance, alumina is a basic material which finds application in a wide variety of processes. The surface chemistry of alumina plays a key role in its performance [10]. Perhaps, the most obvious is its use as catalysts and catalyst supports in the petrochemical industry. Due to the interest in a wide range of catalytic reactions, properties of alumina have been the subject of many investigations [11,12]. However, some fundamentals of alumina surface chemistry are not completely understood yet. Experiments are often difficult to interpret because of the structural complexity of bulk alumina and the difficulty of preparing reproducible well-characterized surfaces. Between the varieties of metastable structures called transition alumina, the most stable form is the α-Al_2O_3, which is the phase studied in the present work.

In the present work, a study of electrostatic charge for α-Al_2O_3 powders with a narrow particle size distribution is performed. Powder parameters and surface characteristics have been taken into account in order to be correlated with the appearance of bipolar charge and elucidate its origin.

2. Experimental method

α-Al_2O_3 powders, alumina powders thereafter, having average particle size range from 0.26 μm to ∼86 μm with a purity >99.5%, and all of them are obtained based on the Bayer method, were studied. The alumina powders were kindly provided by Vicar S.A. (Manises, Spain) [13]. α-Phase (corundum) was selected due to the simple hydrogen-free structure [14].

The specific surface area was measured by the BET method. The particle size distribution was obtained by a laser granulometer (MALVERN MASTERSIZER, Quantacrome, Worcestershire, United Kingdom). The average particle size was determined from the cumulative size of the 50% of particles size distribution, d_{50}, and the Particles Dispersion Index, PDI, was calculated by $PDI = ((d_{90} - d_{10})/d_{50})$, where d_{10} and d_{90} were the particles size distribution for the 10% and 90% of the cumulative particle measurement, respectively. Field emission scanning electron microscopy (FESEM, Hitachi S-4700, Tokyo, Japan) was used to study the particles morphology. The particle diameter and thickness of the particles were determined from the FESEM micrographs with the help of an image analyzer Leika Qwin (Leika Microsystems Ltd., Cambridge, England). The total number of particles measured, extracted from different micrographs at different magnifications, were >500.

Infrared characterization, ATR-IR (Spectrum 100 TF-IR, Perkin Elmer, Massachusetts, USA), was used to study hydroxylation of the particle surface. XPS VG Escalab 200 R (Thermo Fisher scientific, Quebec, Canada) was carried out to obtain the bonding energy of the hydroxyl groups on the alumina surface.

Electrical charge of powder was measured by a double Faraday cup connected to an electrometer (Keithley 6517A, Cleveland, OH, USA). The double Faraday cup consisted of two stainless steel cylindrical cages, of different sizes, concentrically set and isolated to each other by a Teflon® plate. The device is connected to an electrometer which has a particularly high input impedance of 10^{14} Ohm, enough to allow a measurement without disturbing the charge of the object under study, making possible to measure charge as small as pC, which is the order of the noise. The outside cage was grounded to define a reference point. When the powder is dropped in the inner cage an equal charge is induced on the wall of the metallic cylinder. This charge is drawn from the capacitor, C_f, in the feedback loop of the electrometer. The grounded outer cylinder screens out external signals. When a charge is induced a potential is given, Δv_0. The magnitude of the output voltage recorded by the electrometer yields directly the magnitude of the charge, $Q = \Delta v_0 \cdot C_f$, as long as C_f is known. To carry out the charge characterization, the powders were dried at 100 °C for 24 h and were handled with a grounded stainless steel scoop to perform the experiments. Thus, possible tribocharge produced by contact of the single particles with other insulator is negligible by contact of the powder with the grounded scoop. Similar procedure was previously reported [15] as an adequate way to remove the electrostatic charge. The experimental setup included an electronic balance to determine the powder weight; thus, it was possible to normalize the measured charge by the powder mass. The process was repeated 10 times for each powder by using new samples of ∼2 g each time. All experiments were carried out at room temperature and under a relative humidity, R.H., of ∼55–65%. These environmental conditions were the normal working condition used during tests and materials handling.

The surface resistivity of the powders was evaluated by using two points *I–V* curves method. Two factors could contribute to the powders resistivity: (a) the internal resistance, an intrinsic factor that depends on the material structure and (b) the surface resistivity which can depend on other factors as humidity [16]. The dried powders were located in a cylindrical mould made of nylon with two stainless steel press punches, with diameter of 5 cm, which served to transmit the pressure and as electrodes for the used methodology. A force of ∼100 MPa s was applied to allow an adequate contact between particles and electrodes during *I–V* measurements. This pressure was selected because an increment of resistivity was observed for lower pressures due to a possible bad contact between particles. Higher pressures did not change the resistivity value because powder agglomerates broke and the deformation of the compacted ones enters into the elastic regime. At this point the number of the contacts between particles and the condensation of the adsorbed water remain practically constant.

The effect of combining alumina powders with different particle sizes was also evaluated. The weighted powders were located in a nylon cylindrical cage having a volume of 120 cm^3. Dry mixtures of different proportion of two selected alumina powders were performed with a shaker, Mixer-Mill 8000, for 10 min. The use of grinding element was avoided and the energy of the process is low enough to keep the initial particle size and morphology.

3. Results and discussion

The morphology of the different alumina powders is shown in Fig. 1. Table 1 summarizes the main characteristics of the particles obtained from the structural and morphological analyses.

Most of the particles show platelet type morphology. Alumina A powders are formed by large aggregates of stacked platelet like particles with submicron particles attached on the surface, as Fig. 1a illustrates. The rest of alumina powders are formed by individual particles with a nearly hexagonal shape due to the crystalline hexagonal structure.

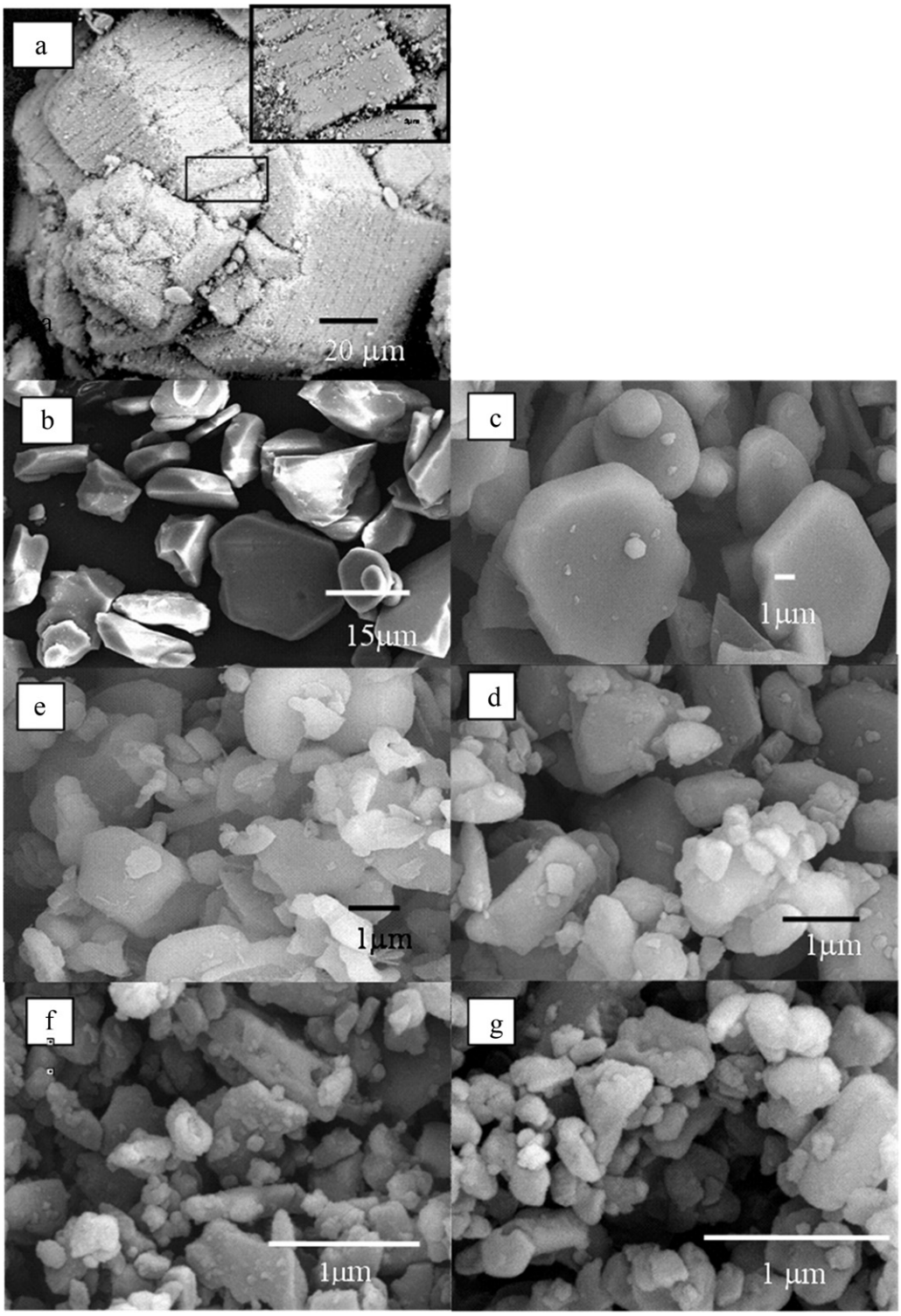

Fig. 1. FESEM micrographs of the different α-Al_2O_3 powders: (a) A (86.46 μm), the inset shown a magnification (b) B (19.65 μm); (c) C (5.91 μm); (d) D (2.78 μm); (e) E (1.36 μm); (f) F (0.86 μm); (g) G (0.26 μm).

Table 1
Parameters of the α-Al_2O_3 powders.

	Alumina powder						
	A	B	C	D	E	F	G
Average particle size ±0.01 (μm)	86.43	19.70	5.91	2.78	1.36	0.86	0.26
Specific surface area ±0.1 (m^2/gr)	0.01	0.1	0.5	1.4	2.6	7.9	8.7
Particle dispersion index ±0.04	1.06	1.03	1.95	3.11	1.72	6.66	2.88
Equivalent particle diameter ±0.1 (μm)	–	19.2	5.4	2.5	1.5	0.4	0.2
Particle thickness ±0.1 (μm)	–	3.4	0.9	0.7	0.2	0.1	0.1
Aspect ratio ±0.3	–	5.6	6.0	3.4	6.1	4.2	3.4

The average particle diameter was measured by laser granulometry after dispersion in aqueous medium. Results, reported in Table 1 show an excellent agreement with the equivalent particle size obtained from FESEM, confirming that the particles are easily de-agglomerated, except for the Alumina F sample, which presents a value about two times higher than the one observed from the micrographs obtained form FE-SEM. This fact indicates that this alumina powder has a higher agglomeration degree than the rest of powders.

FESEM analysis shows that the equivalent particle thickness decreases with the particle size (see Table 1). The variation in aspect ratio indicates changes in the morphology of the particles with a trend to reduce the aspect ratio when the average particle size decreases. This morphology change could provide a different surface for the powders under study.

The specific surface area obtained from BET measurements increases as the average particle size decreases, see Table 1. Fig. 2 shows the specific surface area as a function of the particle size. It can be observed that both curves are very similar except for powder of alumina F, confirming the higher degree of agglomeration of this sample.

The particle dispersion index (PDI), calculated as described above, indicates the broadening of the particles size distribution and serves to evaluate the agglomeration state of the powders with respect to their average particle size. The mentioned index was similar for all the samples but the alumina F which had the largest PDI, as expected by the difference observed between average particle size and specific surface area.

Fig. 3 shows dependence between electrostatic charge and average particle size. The submicronic powders possessed higher electrostatic charge than the largest particles in addition to a bipolarity depending on the particles size. In a first approach, the higher electrostatic charge could be correlated with the specific surface area, but the polarity change was unexplained. The selected alumina powders showed in general good particle dispersion with low agglomeration state, but the handling for the measurement procedure could affect this state. To evaluate the influence of the agglomeration a new set of tribo-charge measurements was performed. The dry powders were slid 10 times by a 50 cm long quartz tube with an inclination of 45°. Fig. 3 shows tribo-charge (●) compared with the net electrostatic charge (○). Both the friction with the quartz tube and the agglomeration of powders increased notably the electrostatic charge except for the alumina E, which maintains a nearly zero electrostatic charge. The charge polarity was maintained during the tribo-generated charge experiments. These results seem to be in accordance with references 2 and 3; however the fact that we are always studying particles of uniform size instead of mixtures of particles with different sizes must be taken into account.

A measurement of the powders resistivity was attempted, Fig. 4. The measured resistivity is in the range of 10^8 Ω cm, which is lower than the one observed for high purity alumina ceramic materials, typically $>10^{14}$ Ω cm [14,17]. The measurements were taken in R.H. of 55–60%; therefore, most of the

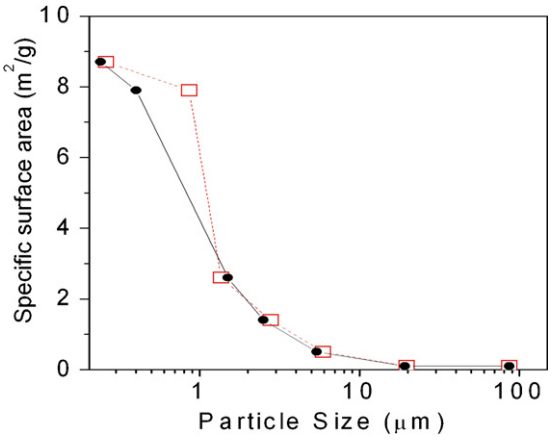

Fig. 2. Specific surface area versus particle size for the different alumina powders (■ average particle size, □ equivalent diameter).

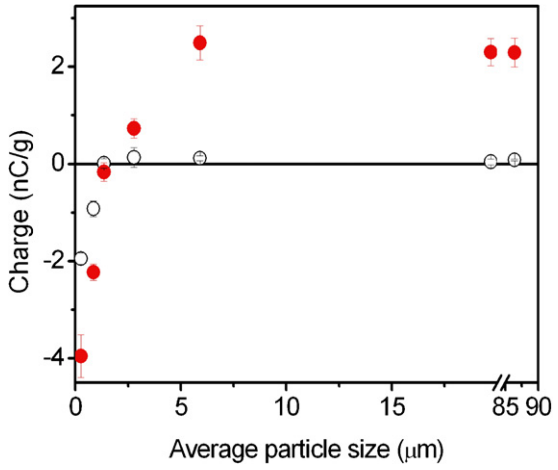

Fig. 3. Intrinsic electrostatic charge (o) and accumulate electrostatic charge (●) for the different average particle size of the alumina powder.

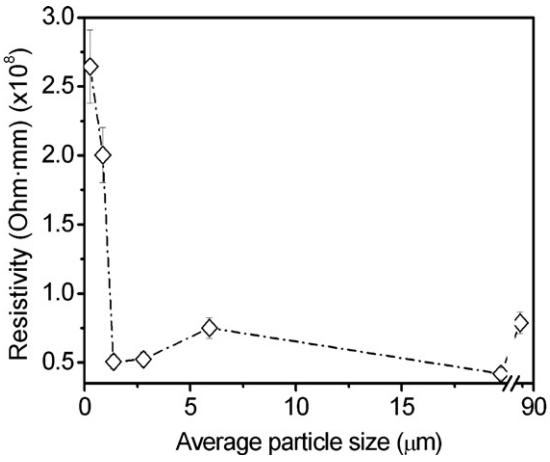

Fig. 4. Resistivity for the different average particle size of the alumina powder.

conduction occurs via the adsorbed water on the different grain surfaces and around the inter-grain contacts [14]. For this reason the measured resistivity can be associated to the surface, as expected. For the submicronic particles the resistivity value was slightly higher due to a higher quantity of water adsorbed by a bigger surface area and, therefore a bigger number of contacts between particles. However, the variations are not relevant enough to explain the differences in electrostatic charge polarity. Thus, the resistivity does not give an explanation about the origin of the charge.

Infrared spectroscopy is an optical technique which can provide information about the chemical structure of the analyzed material by the nature of bonds vibration. Infrared spectroscopy has been shown to be unique for studying the OH groups appearing on the alumina surfaces [18], since the vibration of these groups change as a function of the nature of the adsorbing place at the particle surface. α-Al_2O_3 powders ATR-IR spectra were obtained. Apart from the typical Al–O bonds (not showed here and located below 550 cm^{-1}), the superficial OH groups were observed in the range of 3200–3600 cm^{-1}, Fig. 5. The absorbance of the OH groups is relatively low for all the alumina powders in relation to the vibration of Al–O bonds, as corresponding to high stable surface alumina powders with a small specific surface area.

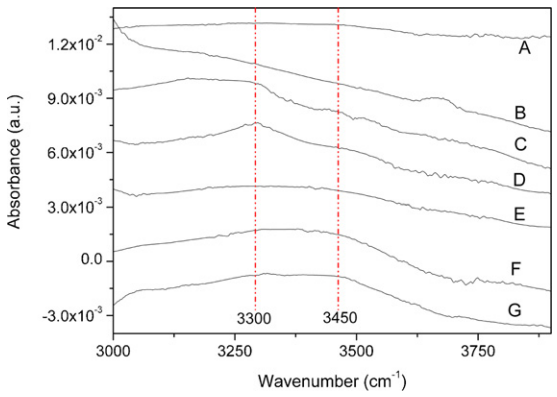

Fig. 5. ATR-IR spectra of alumina powders.

However, changes in the hydroxyl vibration characteristics [13] could be detected by ATR-IR spectra. These changes can be shown through a deconvolution of the bands. Taken into account the mentioned deconvolution it can be seen that the largest particles, alumina powders A and B show lower presence of hydroxyl groups. Alumina powders C and D show mainly hydroxyl groups located at ∼3300 cm^{-1}. Alumina powders F and G show in addition to this peak at 3300 cm^{-1} another contribution at ∼3450 cm^{-1} as can be seen in Fig. 5.

The observed OH groups are generated by a surface hydroxylation, while exposed to air and depending on water partial pressure [19] and the surface structure [20]. Dissociation of H_2O on clean α-Al_2O_3 (0 0 0 1) produces two different types of hydroxyl groups: (a) isolated hydroxyl groups like: O_s–H, that appears at a frequency ∼3430 cm^{-1} (which is detected on our samples), and O_{ads}–H, which should appear ∼3780 cm^{-1}(not detected). Both types of O–H groups present net charge [21], (b) associated hydroxyl groups given as H_2O adhered at the surface, that appear as a broad band at 3200 cm^{-1} [22,23], and contribute to the neutralization of surface charge by hydrogen bonds.

Hence, the hydroxyl groups on the surface can provide a charge and polarity on the powder surface.

In order to corroborate the differences on the hydroxylation, X-ray Photoelectron Spectroscopy, XPS, analysis of alumina C and G powders were performed, Fig. 6. The XPS technique is highly surface-specific due to the short depth penetration of the photoelectrons that are excited from the solid. The technique provides some peaks related to the binding energy of each element which is characteristic for any of them. The shape of each peak and the binding energy can be slightly altered by the chemical state of the emitting atom. Therefore, it is a sensitive technique to detect variations of the adsorbed element at the surface by a variation of the binding energy. As expected the O1s peak shows two contributions, Al–O bonds at 531.4 eV and the contribution of Al–O–H bonds which can appear at different binding energy depending on the OH nature. In sample C this

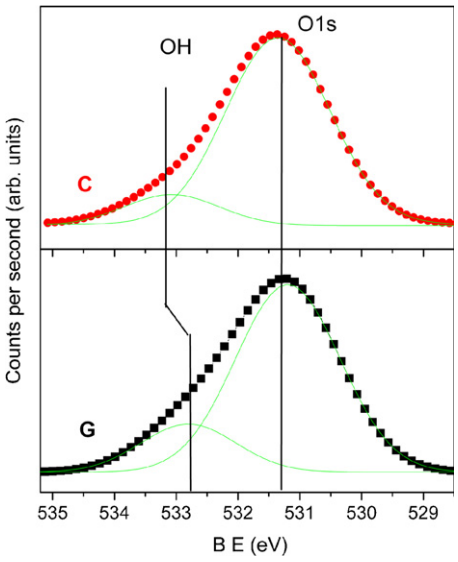

Fig. 6. XPS analysis of alumina powders C and G.

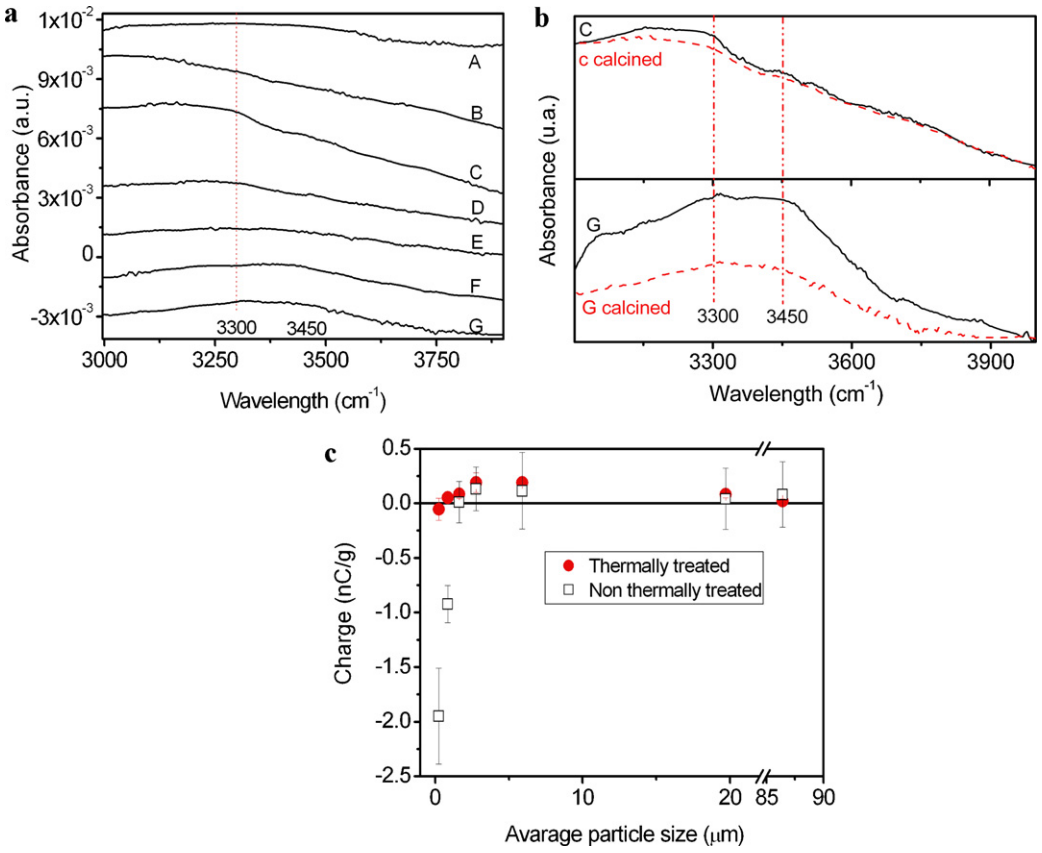

Fig. 7. (a) ATR-IR spectra of 700 °C 1 h thermally treated alumina powders. (b) ATR-IR comparison of the samples A and G before (continous line) and after (dashed line) the thermal treatment. (c) Comparison between intrinsic electrostatic charge of alumina powders before and after a thermal treatment at 700 °C.

contribution appears at 533.25 eV and corresponds to the associated hydroxyl groups. For the sample G, the binding energy is placed at 532.73 eV, related to the presence of both associated and isolated OH groups [24]. According to these assignations, the OH/O ratio of the surface was 0.10 for sample C and 0.28 for sample G. The OH/O ratio variation is expected by the contribution of different type of groups for each sample as observed in ATR-IR spectroscopy, where isolated and associated OH groups were found.

In a first approach, a relationship between the change on the electrostatic charge and the presence of different hydroxyl groups detected by ATR-IR and XPS spectra could be established.

In order to confirm the above-established correlation between superficial hydroxyl groups and intrinsic electrostatic charge, the alumina powders were thermally treated in air at 700 °C for 1 h to modify the surface hydroxyl concentration. This thermal treatment does not change the average particle size for the different alumina powders as an indication that the morphology of the particles remained unaltered, but it was able to remove the surface OH groups. Fig. 7a shows a clear reduction of the peak intensities related to the hydroxyl groups. For clarity, a comparison between two representative samples, C and G, is presented before and after a thermal treatment in Fig. 7b. A larger OH removal is observed for the sample G in comparison to sample C. The net electrostatic charge was measured for the calcined alumina powders and the results were compared to those of the original powders in Fig. 7c. The powders G, particle size ~0.26 μm, showed the larger decreasing of intrinsic charge due to the larger removal of surface O_s–H-groups, which should then be associated to the negative surface charge. However, a small OH removal agrees with the unaltered charge on sample C. Therefore, the nature of the superficial OH-groups is correlated with the intrinsic charge value and polarity on α-Al_2O_3 powders, by the contribution of their charge and the proportion of the different OH groups on the surface.

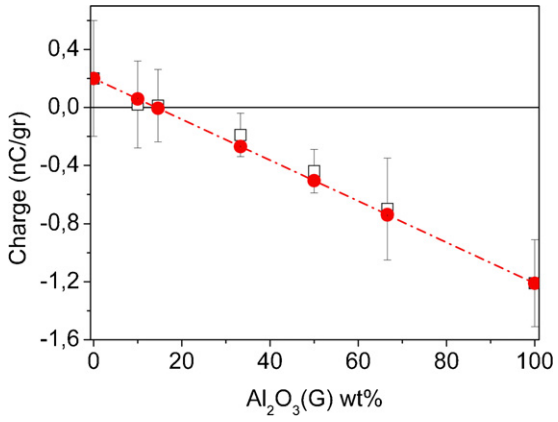

Fig. 8. Intrinsic electrostatic charge of mixtures of alumina powders C (6.13 μm) and G (0.26 μm) (□) and calculated charge (●). by the lever rule calculation.

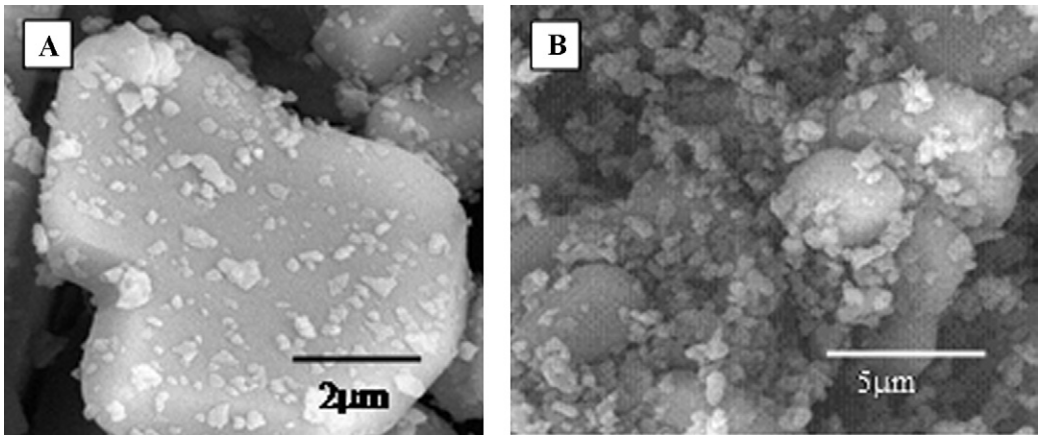

Fig. 9. FESEM micrograph of different weights percentages of alumina powder mixtures. (a) 90/10% of C/G, (b) 50/50% of C/G.

As mentioned before, the powder A, with the biggest average particle size, possesses a distribution of smaller particles dispersed on the surface. This effect is a common situation in powders where small particles were attached to large particles. Based on the above results, differences in electrostatic charge could favour interactions between particles with differences in size and polarity. To explore this phenomenon, mixtures of alumina powders with the same nature but different particles size have been afforded. Electrostatic net charge of the mixtures (□) agrees with the lever rule $Q = ((\text{wt}\%)_C Q_C + (\text{wt}\%)_G Q_G)$ (●), where subscripts denoted the powders used in the mixture, as shown in Fig. 8. Charge compensation was achieved for a given proportion of particles. This effect explains the previous literature difficulties [7] to determine both the value of the electrostatic charge for powders and the origin of such electrostatic charge. In this work, the use of carefully controlled alumina powders served as a case study that allow for the first time in our knowledge to correlate the appearance of electrostatic charge with the surface chemistry of inorganic powders.

In addition to the previous findings, the morphology of the mixtures reveals very interesting features, Fig. 9. Low amount of negatively charged submicronic particles easily dispersed on the surface of the positive large particles. The mixtures were processed by a low energy system as described in the experimental procedure. The dispersion was randomly achieved and it was effective while there were positive sites available. When the concentration of the smallest particles exceeds a certain limit, 10 wt% in this case, an agglomeration of the smallest particles remained and consequently the intrinsic electrostatic charge was negative. This fact could evidence that the particles anchor each other through their surface OH groups [17]. Therefore, charge compensation means a reduction of the surface OH groups and thus, a possible interaction between surfaces. This could be associated with the chemical interaction proposed to be the origin of the appearance of room temperature interphase magnetism observed on particles mixed at low energy and without further thermal treatment [6]. From the technological point of view, a low energy dispersion of particles could represent a new step in the dry dispersion procedures to obtain surface modification characteristic against other methods, such as wet coating which usually modifies the particles by organic additives as dispersants [25] or even dry method with high energy, which leads mechano-synthesis [26]. New findings in the direction of nanoparticles dispersion, nanoparticles handling and contamination could also be derived from the results here reported.

4. Conclusions

A correlation was established, through the study of the surface of the α-Al_2O_3 powders, between net electrostatic charge and surface hydroxylation. The amount and nature of the hydroxyl groups contribute to the electrostatic charge providing its value and polarity.

Bipolarity of fine powders is given by the different nature of the OH groups absorbed on the particles.

The mixtures of particles having intrinsic electrostatic positive and negative charges followed the lever rule. Dry mixtures of differently charged particles favoured the dispersion of a limited amount of smaller particles onto the largest ones. The effective randomly dispersion was achieved by a low energy process that could allow to keep the morphology of the supported particle.

Acknowledgments

This work was supported by the CSIC project PIF MAGIN and by CICYT projects MAT2007-66845-C02-01 and MAT2010-21088-C03-01.

References

[1] J.N. Staniforth, J.E. Rees, Powder Technol. 30 (1981) 255–256.
[2] K.M. Forward, D.J. Lacks, R.M. Sankara, Phys. Rev. Lett. 102 (2009) 028001.
[3] N. Duffa, D.J. Lacks, J. Electrostat. 66 (1–2) (2008) 51–57.
[4] C. Melandri, V. Prodi, G. Tarroni, M. Formignani, T. De Zaiacomo, G.F. Bompane, G. Maestri, in: W.H. Walton (Ed.), Inhaled Particle IV, Pergamon Press, Oxford, UK, 1977, p. 193.
[5] C. Bresges, Nora Anne Urbanetz, Powder Technol. 187 (2008) 260–272.
[6] F. Halima, S.A. Barringer, J. Electrostat. 65 (2007) 168–173.
[7] A.G. Bailey, J. Electrostat. 45 (1998) 85–120.

[8] M.S. Martín-González, J.F. Fernández, F. Rubio-Marcos, I. Lorite, J.L. Costa-Krämer, A. Quesada, M.A. Bañares, J.L.G. Fierro, J. Appl. Phys. 103 (2008) 083905.
[9] Chang, A.J. Kelly, J.M. Crowley (Eds.), Handbook of Electrostic Process1995.
[10] H. Knözinger, P. Ratnasamy, Catal. Rev. Sci. Eng. 17 (1978) 31.
[11] E.P. Reddy, R.S. Varma, J. Catal. 221 (2004) 93–101.
[12] J.T. Richardson, R.M. Scates, M.V.X. Twigg, Appl. Catal. A: Gen. 267 (2004) 35–46.
[13] www.vicar-sa.es/.
[14] I. Levin, D.J. Brandon, Am. Ceram. Soc. 81 (1998) 1995–2012.
[15] M.A. Noras, J. Phys.: Conf. Ser. 142 (2008) 012080.
[16] F. Favrea, F. Villierasa, Y. Duvala, E. McRaeb, C. Rapinb, J. Colloid Interface Sci. 286 (2) (2005) 615–620.
[17] S. Ran, L. Gao, J. Am. Ceram. Soc. 90 (2007) 2626–2629.
[18] X. Liu, R.E. Truitt, J. Am. Chem. Soc. 119 (1997) 9856–9860.
[19] G.V. Franks, Y. Gan, J. Am. Ceram. Soc. 90 (2007) 3373–3388.
[20] J. Goniakowski, C. Noguera, Surf. Sci. 330 (1995) 337–349.
[21] D.B. Mawhinney, J.A. Rossin, K. Gerhart, J.T. Yates, Langmuir 16 (2000) 2237.
[22] K.C. Hass, W.F. Schneider, A. Curioni, W. Andreoni, J. Phys. Chem. B 104 (2000) 5527–5540.
[23] Y. Arai, Chemistry of Powder Production, Chapman and Hall, 1996.
[24] J.T. Kloprogge, L.V. Duong, B.J. Wood, L. Ray, J. Colloid Interface Sci. 296 (2006) 572.
[25] J.F. Fernández, A.C. Caballero, P. Durán, C. Moure, J. Mater. Sci. 31 (1996) 975–981.
[26] R. Pfeffer, R.N. Dave, D. Wei, M. Ramlakhan, Powder Technol. 117 (2001) 40–67.